Article ID: 1003－6326(2004)03－0619－07

Corrosion behavior of two heat treatment Al-Zn-Mg-Cu alloys in different intergranular corrosion solution①

CAO Fa-he(曹发和)[1], ZHANG Zhao(张 昭)[1], LI Jin-feng(李劲风)[1],
CHENG Ying-liang(程英亮)[1], ZHANG Jian-qing(张鉴清)[1, 2], CAO Chu-nan(曹楚南)[1, 2]
(1. Department of Chemistry, Zhejiang University, Hangzhou 310027, China;
2. State Key Laboratory for Corrosion and Protection of Metals, Institute of Metal Research, Chinese Academy of Sciences, Shenyang 110016, China)

Abstract: The electrochemical behavior of two kinds of artificial aged Al-Zn-Mg-Cu alloys in two intergranular corrosion (IGC) solutions were studied using electrochemical impedance spectroscopy (EIS) and open circuit potential (OCP) at steady-state. EDAX result indicates that different artificial ageing methods change the composition and content of Cu and Zn in different zones. Zn/Cu depleted precipitation-free zone that plays a very important role in IGC is formed by heating the solubilized Al alloy for 135 ℃ at 16 h. All impedance spectra of the two alloys in two IGC solutions can be divided into three types. The two different states Al alloys takes on one time constant and two capacitive arcs at high-mediate frequency and low frequency in the NaCl+ $(NH_4)_2SO_4$ solution respectively; but in the NaCl+ HCl solution, impedance displays one capacitive arc at the high-mediate frequency and an inductive loop at low frequency. OCP results show that more micro-galvanic cells in the NaCl+ $(NH_4)_2SO_4$ solution than that in the NaCl+ HCl solution results in more potential fluctuation amplitude, and long-term drift of OCP is due to the long-term variation of the cathodic and anodic corrosion processes.

Key words: intergranular corrosion(IGC); Al-Zn-Mg-Cu alloy; electrochemical impedance spectroscopy; electrochemical noise; morphology

CLC number: TG 174 **Document code:** A

1 INTRODUCTION

Aluminum is one of the most abundant elements in nature. It is of low density, high elasticity, high thermal and electrical conductivity, high corrosion resistance, and high capacity to form alloys with many elements, which makes it one of the most useful materials in construction and aerospace industry. Alloying elements such as copper and zinc may lower the corrosion resistance of Al alloy, whilst the heat treatment can change susceptibility of the alloy to different types of localized attack (pitting, intergranular corrosion, exfoliation, etc). Among all aluminum alloys, Al-Zn-Mg-Cu alloy is widely applied to airplane structure due to its excellent mechanical properties[1, 2], but it often exhibits structural corrosion such as intergranular corrosion, which lowers the strength and plasticity, the fatigue property, and decreases the service life[3-5].

It is generally thought that the intergranular corrosion is developed from a local corrosion cell, with the copper-depleted precipitation-free zone (PFZ) along the grain boundaries (GB) being the anode, and the grain particles (GP) and the intermetallic being cathodes for the Al-Cu alloy[6]. The intergranular corrosion would then be a process in which a very small anode is in contact with a large cathode. Colner et al[7] believed that during corrosion process the potential difference is about 100 mV. Whereas, the mechanism of anodic and cathodic zones does not illuminate the effect of aggressive ions on the intergranular corrosion, and the intergranular corrosion should occur in almost any corrosive medium[8]. However, our works show that the Cl^- or/and SO_4^{2-} is not the effective aggressive ions to initiate intergranular corrosion and exfoliation corrosion in the Al-Zn-Mg-Cu alloy[9-11].

Meanwhile, electrochemical techniques (EIS and EN) have been widely used to study the corrosion process[6, 8, 12-15], but they devoted their attention to detect the corrosion of alloys, not to study the relationship between the corrosion and electrochemical

① **Foundation item:** Project (G19990650) supported by the National Key Fundamental Research and Development Program of China; project (50271066) supported by the National Natural Science Foundation of China; project supported by the State Key Laboratory for Corrosion and Protection, China

Received date: 2003－03－10; **Accepted date:** 2004－03－10

Correspondence: CAO Fa-he, PhD; Tel: +86-571-87952318; E-mail: caofh9@sohu.com

features. Therefore, we use the electrochemical technique and morphology detected to study the intergranular corrosion behavior of Al-Zn-Mg-Cu alloy in this paper, try to illustrate the effect of aggressive ions on its corrosion process, and to find some regular relationship between the intergranular corrosion and the electrochemical features during the corrosion process and develop the electrochemical method for evaluating intergranular corrosion quantitatively and quickly.

2 EXPERIMENTAL

Commercial Al-Zn-Mg-Cu alloy was from institute of Beijing Aeronautics and Astronautics Research. The mass fractions(%) of the aluminum alloy are Zn 5.71, Mg 2.42, Cu 1.63, Cr 0.19, Fe 0.30, Mn 0.08 and Si 0.015. Specimen sheets of 5 mm thick were cut from larger sheet. The solubilized Al-Zn-Mg-Cu alloy was prepared by heating the specimens at 470 ℃ for 40 min, then water quenched. The aged specimens were prepared by heating the solubilized specimens at 121 ℃ for 35 h, then at 160 ℃ for 20 h(state A); and the other aged specimens were obtained by heating the solubilized material at 135 ℃ for 16 h(state B). Before being tested, the specimens were connected to a copper wire, and then mounted in epoxy resin with only one surface (4 cm^2) exposed. The exposed surface was grinded using abrasive papers from 500# to 1 200#, polished with diamond paste, degreased using acetone, rinsed with water and dried in air.

The IGC solutions were prepared with analytical grade reagents and twice-distilled water, and according composition is listed in Table 1.

Table 1 Composition of two IGC solutions

Electrolyte	ρ_{NaCl}/ ($g \cdot L^{-1}$)	$\rho_{(NH_4)_2SO_4}$/ ($g \cdot L^{-1}$)	c_{HCl}/ ($mol \cdot L^{-1}$)
IGC one	35	5	–
IGC two	30	–	10

The initial pH value of the two solutions were 5.00 and 0.63 respectively and the solution temperature was maintained at 25 ℃ using a thermostat.

The as-test specimens were continuously immersed in a three compartments, exposing metal surface of 1 cm^2 to approximately 20 mL IGC solution for 24 h. Two artificial aged Al alloy plates were used as the working electrode, and a large platinum sheet and a saturated calomel electrode (SCE) with a luggin capillary were severed as the counter and the reference electrode respectively. All mentioned potentials were referred to the saturated calomel electrode (SCE). Electrochemical impedance spectroscopy (EIS) measurement was performed with a model 273A (Princeton Applied Research) on the corrosion potential and always taken in the direction of decreasing frequency. EIS experiments were carried out using a three compartment. A frequency range of 1×10^5 to 5×10^{-2} Hz was selected for its sensitivity to corrosion resistance; a sinusoidal perturbation of 10 mV rms was employed in all cases. Then the morphology was identified by SEM and metalloscope. Meanwhile, the EIS data were simulated using ZView program. The electrochemical noise testing configuration is the common three-electrodes system too. Electrochemical noise measurements were carried out on a CHI660A, a product of CH Instruments, Inc. (3700 Tennison Hill Drive l Austin, TX 78738 l USA), and the sampling interval used in this study is 0.1 s. At the end of immersion, the working electrode was put out, washed by distilled water, dried in a stream of hot air, then detected using metalloscopy and SEM. In order to see the morphology of the corroded specimen surface clearly, the corrosion product was removed by 2% CrO_3 + 5% H_3PO_4 solution at 80 ℃[16].

3 RESULTS AND DISCUSSION

3.1 EDAX results of Al-Zn-Mg-Cu alloys

Specimens of two kinds of artificial aged Al-Zn-Mg-Cu alloy were immersed in Kuller Reagent (HF 1.0 mL; HCl 1.5 mL; HNO_3 2.5 mL; H_2O 95 mL) for 55 s to distinguish grain boundaries (GB) and grain particles (GP) zone. From the SEM image, it can be seen that state B alloy has formed some intermetallic compound in GB zone, and the GB zone is long and narrow for state A while it is broad for state B. The EDAX and SEM experiments results are as follows.

1) The contents of zinc and copper in GB zone are higher than those in GP zone. These two state alloys have similar results.

2) The copper content in GP zone for state A is less than that for state B, but the zinc content is almost the same. The copper and zinc content in GB zone are almost the same too (state A: without intermetallic compound).

3) For state B, there is some intermetallic compound in GB zone, and the contents of zinc and copper of intermetallic compound are much higher than those in GP zone and around intermetallic compound. The copper-zinc-depleted precipitation-free zone is formed along the grain boundaries.

3.2 Electrochemical experiment results

3.2.1 State A in 35 g/L NaCl + 5 g/L $(NH_4)_2SO_4$

The Al-Zn-Mg-Cu alloy of state A was immersed in 35 g/L NaCl + 5 g/L $(NH_4)_2SO_4$ solution for 24

h, and corresponding impedance spectroscopy was measured at different time. The impedance spectra of 24 h is shown in Fig. 1. During the whole immersion period, only a visual depressed capacitive arc above the real axis can be observed. The maximal phase angle is close to − 80°, which indicates the sample surface has a homogeneous interface. In the whole immersion process, there is not any change at the surface of specimen observed by eyes. At the metalloscope, there are several very small pits for whole surface (4 cm^2) which can not be detected by EIS, so the Bode and Nyquist plot take on one time constant which is corresponding to double-layer.

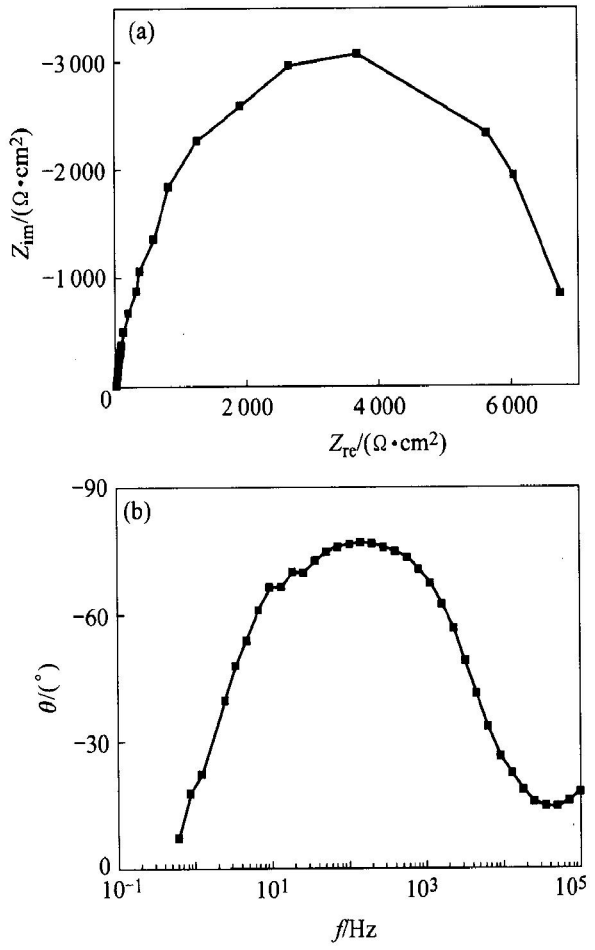

Fig. 1 Evolution of Nyquist(a) and corresponding Bold(b) diagram after 24 h immersion
(State A alloy immersed in 35 g/L NaCl+ 5 g/L $(NH_4)_2SO_4$ solution)

The profile of the open circuit potential (OCP) vs time is shown in Fig. 2 for state A alloy electrode in the IGC solution during the whole immersion time. The maximal fluctuation of OCP is no more than 15 mV. The OCP is − 0.674 V at the begining of immersion, and becomes more negative and gets the minimal value at immersion for 4 h, then keeps a balance at − 0.675 V until 16 h immersion, then has a positive shift, and the final stable OCP is the same as the initial OCP.

3.2.2 State A alloy in 30 g/L NaCl+ 10 ml/L HCl

After immersed for 15 min, several little bubbles appeared on the working electrode surface, and the bubbles became larger with time, adsorbed tightly on the electrode surface. At the beginning of immersion, the OCP has about 10mV fluctuation and the fluctuation of OCP became less with time. Typical Nyquist plots are shown in Fig. 3. The Nyquist plots is composed of a depressed capacitive arc and an inductive loop, the radius of capacitive arc increases and the inductive loop decreases during the whole immersion time.

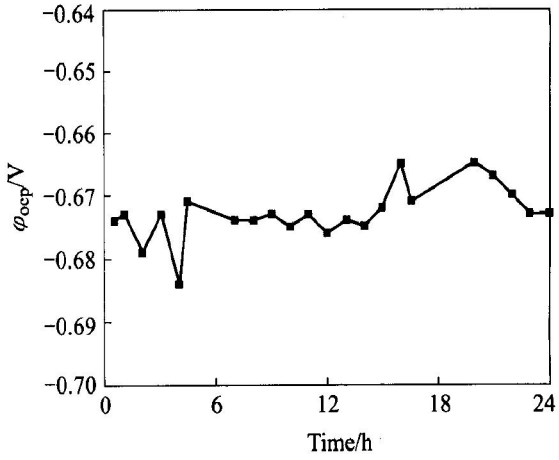

Fig. 2 Variation of open circuit potential(φ_{OCP}) of state A alloy electrode with time in 35 g/L NaCl + 5 g/L $(NH_4)_2SO_4$ solution

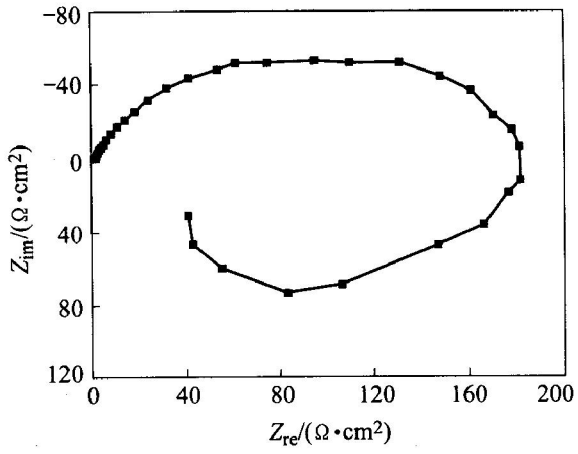

Fig. 3 Evolution of Nyquist plots of state A alloy after immered in 30 g/L NaCl+ 10 mL/L HCl solution for 24 h

3.2.3 State B alloy in 35 g/L NaCl + 5 g/L $(NH_4)_2SO_4$

Typical impedance (Nyquist and Bold plots) curves are shown in Fig. 4, which are corresponding to immersion time of 24 h. Though the visual evaluation of the impedance date on the Nyquist plot obtained in the whole frequency yield only one time constant; but from the Bode plot, there are obvious two capacitive arcs in high-mediate frequency and low fre-

quency, and the maximal phase angel is close to −72°. Before immersed for 4 h, the impedance curve is just like that in Fig. 1, and the only difference is radius of capacitive arc above real axis at the Nyquist plot. The EIS data above the real axis at different immersion times are analyzed with ZView program using the equivalent circuit as shown in Fig. 5, which is based on the comprehension of the IGC process.

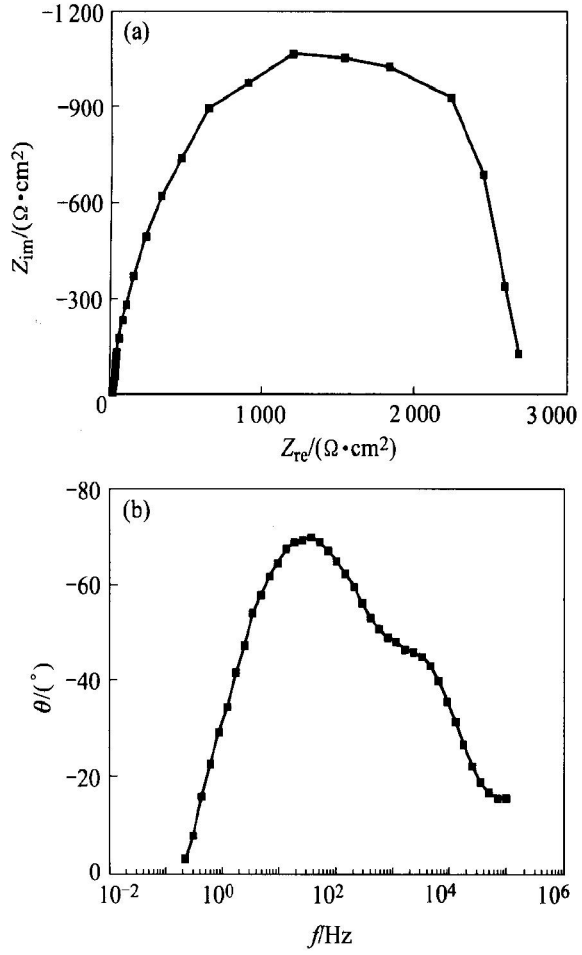

Fig. 4 Evolution of Nyquist(a) and corresponding Bold(b) diagram of state B alloy immersed in 35 g/L NaCl + 5 g/L $(NH_4)_2SO_4$ solution for 24 h

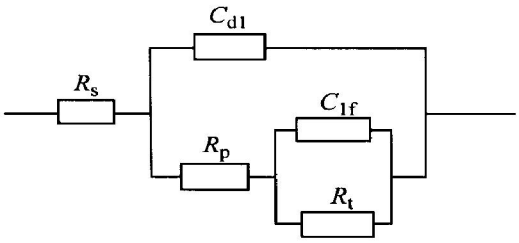

Fig. 5 Equivalent electrical circuit for immersion of Al-Zn-Mg-Cu alloy in IGC solution (R_s: solution resistance; C_{dl}: origin surface double layer capacitive; R_p: polarization resistance; C_{lf}: low frequency capacitive; R_t: charge transfer resistance)

The profile of OCP vs time is shown in Fig. 6 for state B alloy electrode in IGC solution during the whole immersion time. The OCP increases gradually from − 0.796 V to − 0.770 V at the first 5 h-immersion, then keeps less fluctuation around the OCP and arrives at − 0.760 V at the end of immersion.

3.2.4 State B alloy in 30 g/L NaCl+ 10 ml/L HCl

There are several hydrogen bubbles on the electrode surface at the immersion for 10 min, and the experiment phenomenon in whole immersion time is just like that of the state A alloy in 30 g/L NaCl+ 10 ml/L HCl solution. Fig. 7 illustrates the Nyquist plot for state B alloy after immersed in 30 g/L NaCl+ 10 mL/L HCl solution for 24 h. As can been seen, one depressed capacitive loop in the high-mediate frequency range and an inductive loop in low frequency range are observed. With the immersion prolonging, the radius of capacitive loop increases to about 3.0 $\Omega\cdot cm^2$ at the end of immersion, which is much lower than that in 35 g/L NaCl+ 5 g/L $(NH_4)_2SO_4$ solution.

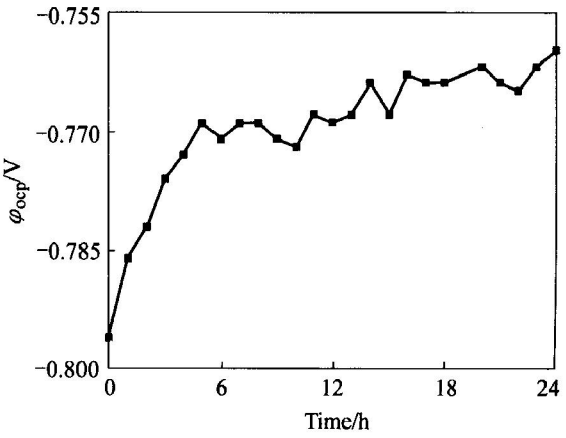

Fig. 6 Variation of open circuit potential(φ_{OCP}) with time for state B alloy electrode in 35 g/L NaCl + 5 g/L $(NH_4)_2SO_4$ solution

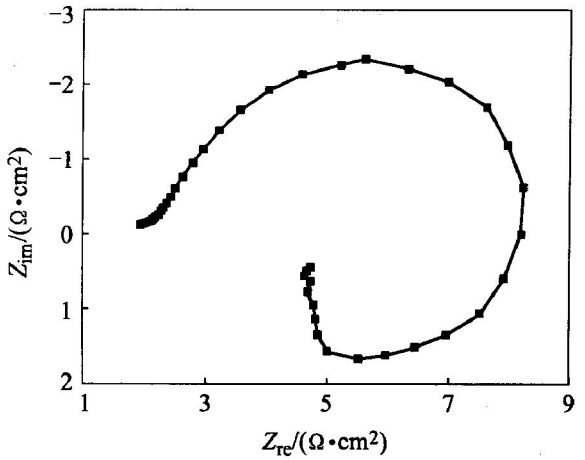

Fig. 7 Evolution of Nyquist plot of state B alloy after immersed in 30 g/L NaCl+ 10 mL/L HCl solution for 24 h

The typical cross-sectional metallograph of state B alloy in 35 g/L NaCl+ 5 g/L $(NH_4)_2SO_4$ solution after immersed for 24 h is shown in Fig. 8. The analogical IGC images of other alloys in different IGC solutions are just like that in Fig. 8.

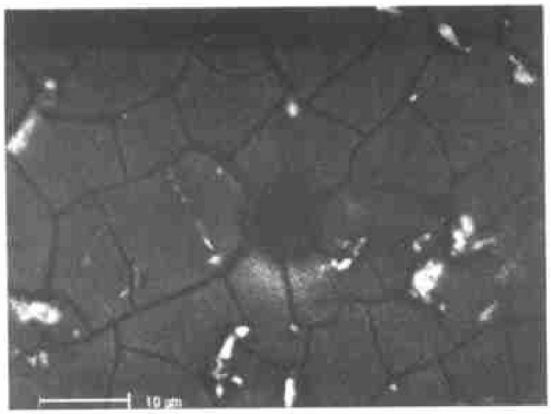

Fig. 8 Typical cross-sectional metallograph of state B alloy after immersed in 35 g/L NaCl + 5 g/L $(NH_4)_2SO_4$ solution for 24 h

3.3 Discussion

The variation of the open circuit potential (OCP) with time can give an indication of the anodic and cathodic reaction. Fig. 9 interprets how the micro-galvanic cells on the corroding surface affect the potential at position "p" in solution, where the sign "±" represents a micro-galvanic cell. From the EN (continuous OCP, sampling frequency 10 Hz) experiment, the fluctuation amplitude in NaCl+ HCl solution is lower than that in NaCl+ $(NH_4)_2SO_4$ solution, which indicates that there are more micro-galvanic cells in NaCl+ $(NH_4)_2SO_4$ solution than that in NaCl+ HCl solution. It is in accord with the EDAX results. The fluctuation of OCP characterized by the repetitions in which the OCP suddenly drops negatively and instantly restores positively. As discussed above, the numerous micro-galvanic cells on the corroding electrode may cause this, while the long-term drift of OCP may be a result of the long-term variation of the cathodic and anodic corrosion processes. This can be illustrated by Evans diagram of Fig. 10, where the increase in cathodic polarization causes the free corroding potential to move from φ_{corr1} to φ_{corr2} and the anodic polarization cause the potential to drift from φ_{corr1} to φ_{corr3}. In the case of state B alloy in NaCl+ $(NH_4)_2SO_4$ solution, the Zn/Cu depleted precipitation-free zone are the sites for anodic reaction, and the total cathodic area are apparently smaller than anodic area (the matrix). So the corrosion process is under anodic control. As the immersion time prolongs, the cathodic and anodic reaction will keep balance, therefore, the open circuit potential will keep balance as well (see Fig. 6). In the case of state A alloy in NaCl+ HCl solution, because of the hydration of the surface aluminum atoms, the OCP will drift in the negative direction. On the other hand, the cathodic reaction on the surface of Al-Zn-Mg-Cu alloy (main reaction is the reduction of hydrogen) can take place on the whole electrode surface, while the anodic process (the dissolution of the Al^{3+}) can take place only on the spot where the passive film has already broken down. It is obvious that the anodic area is much smaller than the cathodic one; and the corrosion process is under anodic control. Because the passive film of aluminum will breakdown or repassivate, the total anodic area will change with the time, which will obviously cause the long term fluctuation of the OCP. The hydrogen will be exhausted with time, so at the retral immersion time, there are some positive direction shift in Fig. 2.

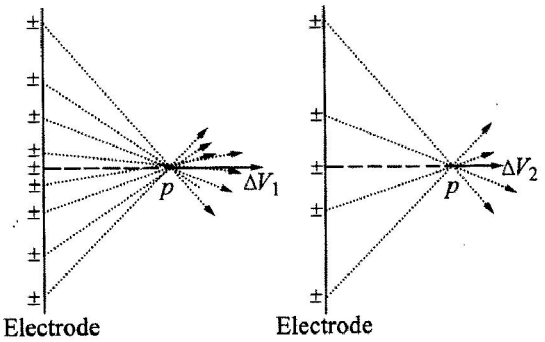

Fig. 9 Schematic illustration of ways of micro-galvanic cells affecting potential at position "p" ($\Delta V_1 > \Delta V_2$)

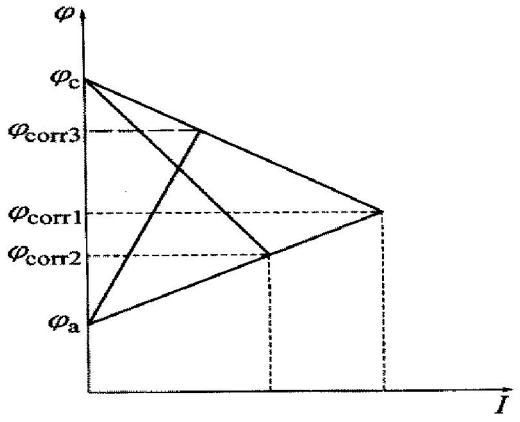

Fig. 10 Schematic illustration of variations in cathodic or anodic activity causing drift of open circuit potential

From the EIS experiment, all impedance spectra of two heat treatments in two IGC solutions can be divided into three types as follows.

1) Only one capacitive during the whole frequency range. The state A alloy in NaCl+ $(NH_4)_2SO_4$ solution takes on only one time constant. At the end of immersion, there are several little pits on the electrode surface, which couldn't be detected by EIS, so there is only one capacitive arc that corresponds to the double layer. The radius of capacitive arc has no re-

markable change because of no obvious change of electrode surface during the whole immersion time.

2) One capacitive arc at the high-mediate frequency and an inductive loop at the low frequency. Two states Al alloys in the NaCl+ HCl solution display EIS features just like this. At the end of the immersion, there is IGC on the electrode surface from the metalloscopy detection. The inductive behavior is often explained by the relaxation phenomenon of reaction intermediates[17]. In fact, the origin of inductive features is numerous. For example, when the electrode potential shifts towards more anodic direction and if the time dependent change of the electrode interface promotes the dissolution reaction (or conversely the cathodic potential shifts to the cathodic process), an inductive feature is expected. On this point, it is believed that the inductive loop is associated with the weakening of the protective effectiveness of the aluminum oxide layer due to the anodic dissolution of aluminum alloy. With prolonging the immersion time, the surface oxide layer becomes progressively less protective, due to the action of the aggressive anions in the IG solution. Then, the relaxation of weak points diminishes and the low frequency inductive loop will be weakened. It is obvious that the capacitive arc is corresponding to the original surface and the inductive loop is corresponding to the reaction information. The inductive loop shrinks with time, which indicates that the surface is attacked more severely with the increase of the immersion time[17], due to the action of the aggressive anions in the IG solution.

3) Two capacitive arcs at different frequency zone. The state B alloy in NaCl+ $(NH_4)_2SO_4$ solution presents two time constant features. The high-mediate frequency capacitive arc originates from the original corroded surface, while the mediate-low frequency one is corresponding to the new surface by IG attack, which results in IGC. Through the equivalent electrical circuit as shown in Fig. 5, the low frequency capacitive value vs. time is shown in Fig. 11. As can be seen in Fig. 11, the C_{lf} gets the lowest value at 4 h immersion, and then shifts upward slowly. This phenomenon is corresponding to the repassivation of interface film. In NaCl+ $(NH_4)_2SO_4$ solution, the pit attack is prior to occur and the repassivation process occurs at the same time. There is a couple of competition reaction. Repassivation process is the main factor at the first 4 h immersion, and at the remanent time, the IG attack is the main process, so at the end of immersion, there is only a visible IG morphology.

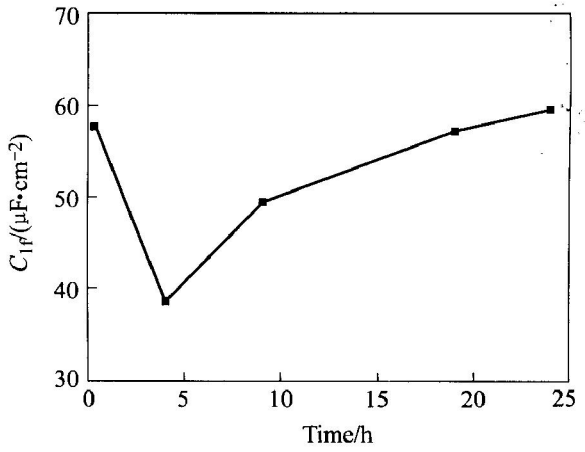

Fig. 11 C_{lf} as function of immersion time of state B alloy in 35 g/L NaCl + 5 g/L $(NH_4)_2SO_4$ solution

It is generally considered that pitting corrosion occurred first and then the corrosion chimneys maintained the acidic, chloride pit environment that subsequently caused IGC (preferential dissolution of the region adjacent to the grain boundaries)[8]. From the EDAX results, artificial ageing changes the composition and element content of different zone. The Zn/Cu depleted precipitation-free zone is formed by the second heat treatment, which plays a very important role for the IGC in the NaCl+ $(NH_4)_2SO_4$ solution (IGC in neutral solution). Al has a more active potential (solution potential) than Cu and Zn, so the Cu/Zn depleted zone dissolve preferentially in IGC solutions, which is adjacent to the GBs. But in the NaCl+ HCl solution, the initial pH value is very low (pH= 0.63) and the evolution of hydrogen plays an important role in the IG corrosion.

The main difference of the two kind IGC solution is that the proton concentration, and the aggressive ion, just like Cl^-, is at the same quantity. From our prevenient works, the SO_4^{2-} is not an effective aggressive ion to initiate a pitting or intergranular corrosion. So Neutral solution (NaCl+ $(NH_4)_2SO_4$) alone did not attack the depleted regions along the grain boundaries of A kind heat-treated Al-Zn-Mg-Cu alloy, but attacked the depleted regions preferentially of kind B heat treatment alloy, and occurred IG corrosion. The preferential attack of the GBs region occurred instead in acidic environment (NaCl+ HCl) of two kind heat treatments alloys. In neutral solution, the Cl^- and/or SO_4^{2-} are not an effective aggressive ion of IG corrosion, but the proton, which combines with aggressive ion, is the most important factor of IG corrosion. In neutral solution, NH_4^+ plays an important role in improving IGC by forming complex with many transition metals, just like Cu, Zn. So we consider that NH_4^+ dissolves the Cu and Zn preferen-

tially on the GBs of kind B heat treatment. There are two kinds of attack of Al-Zn-Mg-Cu alloy in two IG solutions.

4 CONCLUSIONS

1) Electrochemical impedance spectroscopy is a convenient technique to study the intergranular corrosion process, and can provide the corrosion detail and corrosion dynamics.

2) All impedance spectra of two heat treatment alloys in two IGC solutions can be divided into three types. When intergranular corrosion occurs in NaCl+ $(NH_4)_2SO_4$ solution, the mediate-low frequency capacitive loop comes forth and bode plot is mainly composed of two capacitive arcs. The high-mediate one originates from the old surface of the corroding electrode while the low frequency loop from the newly formed interface by intergranular corrosion. In NaCl + HCl solution, the low frequency inductive loop is corresponding to the IGC information and shrinks with time, which indicates that the specimen surface is attacked more severely with immersion time.

3) Different heat treatment and different IGC solution result in different corrosion modality, including pitting and intergranular corrosion, which corresponds with different EIS feature. In NaCl + $(NH_4)_2SO_4$ solution, the Cu/Zn depleted precipitation-free zone plays an important role in IGC, but in NaCl+ HCl solution, the proton, which combines with the aggressive ion, is a more important factor to occur IGC.

REFERENCES

[1] Robinson M J, Jackson N C. Exfoliation corrosion of high strength Al-Cu-Mg alloys: effect of grain structure [J]. British Corrosion Journal, 1999, 34(1): 45 - 49.

[2] de Daborenea J, Conde A. Intergranular corrosion of 8090 Al-Li: interpretation by electrochemical impedance spectroscopy[J]. British Corrosion Journal, 2000, 35 (1): 48 - 53.

[3] HE Jian-ping, CHEN Wen-li, XU Wei, et al. Effect of exfoliation on structure and tensile strength of LC4CS aluminum alloy at constant temperature[J]. Journal of Nanjing University of Aeronautics and Astronautics, 1999, 31(5): 575 - 579.

[4] HE Bin, SUN You-chao, FAN Wei-xun. Influence of exfoliation corrosion on the fatigue of aluminum alloy[J]. Journal of Nanjing University of Aeronautics and Astronautics, 1998, 30(3): 306 - 310.

[5] Kelly D J, Robinson M J. Influence of heat treatment and grain shape on exfoliation corrosion of Al-Li alloy 8090[J]. Corrosion, 1993, 49(10): 787 - 795.

[6] Conde A, de Damborenea J. An electrochemical impedance study of a natural aged Al-Cu-Mg alloy in NaCl[J]. Corrosion Science, 1997, 39(2): 295 - 303.

[7] Colner W H, Francis H R. A contribution to the theory of stress corrosion in Al-4% Cu alloys[J]. Journal of Electrochemistry Society, 1958, 105(7): 377 - 384.

[8] Galvele J R, de Micheli S M. Mechanism of intergranular corrosion of Al-Cu alloys[J], Corrosion Science, 1970, 10(6): 795 - 807.

[9] Cao F H, Cheng Y L, Zhang Z, et al. Features of electrochemical noise during pitting corrosion of LC4 aluminum alloy in 2.0% NaCl solution[J], The Chinese Journal of Nonferrous Metals, 2002, 12(1): 245 - 249. (in Chinese)

[10] Cao F H, Zhang Z, Cheng Y L, et al. Eletrochemical noise features of pure aluminum during pitting corrosion in neutral NaCl solution[J]. Acta Sinca Metallic, 2003, 16(1): 22 - 27.

[11] Cao F H, Zhang Z, Cheng Y L, et al. Eletrochemical features during pitting corrosion of LY12 aluminum alloy in different neutral solutions[J]. Acta Sinca Metallic, 2003, 16(4): 319 - 326.

[12] LI Di, HU Yang-ling, GUO Bao-lan. Study on the evaluation of localized corrosion of 2024T3 aluminum alloy with EIS[J]. Mater Sci Eng, 2000, A280: 173 - 176.

[13] Tanguy D, Bayle B, Dif R, et al. Hydrogen effects during IGSCC of pure Al-5Mg alloy in NaCl media[J]. Corrosion Science, 2002, 44(8): 1163 - 1175.

[14] Christopher M, Brett A. On the electrochemical behavior of aluminum in acidic chloride solution[J]. Corrosion Science, 1992, 33(2): 203 - 210.

[15] Burleigh T D, Ludwiczak E, Petri R A. Intergranular corrosion of an aluminum-magnesium-silicon-copper alloy [J]. Corrosion, 1995, 51(1): 50 - 55.

[16] William H C. Metals Handbook. Surface Cleaning, Finishing and Coating[M]. 9th ed, Vol. 5, Metals Park, OH: ASM Int, 1982. 8 - 9.

[17] Keddam M, Kuntz C, Takenouti H, et al. Exfoliation corrosion of aluminum alloys examined by electrode impedance[J]. Electrochim Acta, 1997, 42(1): 87 - 97.

(Edited by LONG Huai-zhong)